Sulforaphane Causes Autophagy to Inhibit Release of Cytochrome *c* and Apoptosis in Human Prostate Cancer Cells

Anna Herman-Antosiewicz, Daniel E. Johnson, and Shivendra V. Singh

Department of Pharmacology and University of Pittsburgh Cancer Institute, University of Pittsburgh School of Medicine, Pittsburgh, Pennsylvania

Abstract

The present study reports a novel response to sulforaphane, a highly promising anticancer constituent of several edible cruciferous vegetables, in PC-3 and LNCaP human prostate cancer cells involving induction of autophagy. Exposure of PC-3 and LNCaP cells to sulforaphane resulted in several specific features characteristic of autophagy, including appearance of membranous vacuoles in the cytoplasm as revealed by transmission electron microscopy and formation of acidic vesicular organelles as revealed by fluorescence microscopy following staining with the lysosomotropic agent acridine orange. The sulforaphane-induced autophagy was associated with up-regulation, processing, and recruitment to autophagosomes of microtubule-associated protein 1 light chain 3 (LC3), which is a mammalian homologue of the yeast autophagy regulating protein Apg8/Aut7p. Treatment of cells with a specific inhibitor of autophagy (3-methyladenine) attenuated localization of LC3 to autophagosomes but exacerbated cytosolic release of cytochrome *c* as well as apoptotic cell death as revealed by analysis of subdiploid fraction and cytoplasmic histone–associated DNA fragmentation. In conclusion, the present study indicates that induction of autophagy represents a defense mechanism against sulforaphane-induced apoptosis in human prostate cancer cells. To the best of our knowledge, the present study is the first published report to convincingly document induction of autophagy by an isothiocyanate class of dietary chemopreventive agent. (Cancer Res 2006; 66(11): 5828-35)

Introduction

Epidemiologic data continues to support the premise that dietary intake of cruciferous vegetables may be protective against the risk of different types of malignancies, including cancer of the prostate (1–4). Organic isothiocyanates, which occur naturally as thioglucoside conjugates (glucosinolates) in a variety of edible cruciferous vegetables, including broccoli, are believed to be responsible for anticancer effects of cruciferous vegetables (reviewed in refs. 5, 6). Organic isothiocyanates are generated due to myrosinase-mediated hydrolysis of corresponding glucosinolates (5, 6). Sulforaphane [1-isothiocyanato-4-(methylsulfinyl)-butane] is a naturally occurring member of the isothiocyanate family of chemopreventive agents that has generated a great deal of research interest due to its interesting biological effects (7–10). For example, sulforaphane is a potent inducer of the expression of glutathione transferases, which are responsible for detoxification of activated intermediates of a variety of environmental carcinogens, including polycyclic aromatic hydrocarbons (7, 11). In addition, sulforaphane is an inhibitor of CYP2E1, which is involved in the activation of carcinogenic chemicals (12). Cancer chemoprevention by sulforaphane or its *N*-acetylcysteine conjugate has been observed against 9,10-dimethyl-1,2-benzanthracene–induced mammary cancer in rats (8), azoxymethane-induced colonic aberrant crypt foci formation in rats (9), and benzo(*a*)pyrene-induced forestomach cancer in mice (10).

More recent studies have revealed that sulforaphane inhibits proliferation of cultured cancer cells by causing G_2-M phase cell cycle arrest and/or apoptosis induction (13–20). The *N*-acetylcysteine conjugate of sulforaphane was recently shown to inhibit histone deacetylase activity (21). Orally administered sulforaphane at concentrations that may be generated through dietary intake of cruciferous vegetables significantly suppressed growth of PC-3 xenografts in athymic mice without causing weight loss or any other side effects (17).

An understanding of the mechanism by which sulforaphane causes cell cycle arrest and apoptosis induction in cancer cells is critical for its further development as a clinically useful cancer preventive/therapeutic agent because this knowledge could lead to identification of mechanism-based biomarkers potentially useful in future clinical trials. Recent studies from our laboratory have offered novel insights into the mechanism of sulforaphane-induced cell cycle arrest and apoptosis induction (17–20). Using human prostate cancer cells as a model, we have shown that the sulforaphane-mediated G_2-M phase cell cycle arrest is associated with checkpoint kinase 2–mediated phosphorylation of Cdc25C at Ser^{216} leading to inactivation of cyclin-dependent kinase 1 (18), which together with the B-type cyclins plays an important role in regulation of G_2-M transition. More recent studies from our laboratory have revealed that the caspase-dependent apoptosis resulting from sulforaphane treatment is regulated by Bax and Bak and initiated by generation of reactive oxygen species leading to disruption of the mitochondrial membrane potential and cytosolic release of cytochrome *c* (19, 20).

The present study reports a novel response to sulforaphane in PC-3 and LNCaP human prostate cancer cells involving formation of acidic vesicular organelles (AVO) and autophagy. The sulforaphane-induced autophagy in PC-3/LNCaP cells is associated with up-regulation and processing of autophagy-related protein microtubule-associated protein 1 light chain 3 (LC3) and its recruitment to the autophagosomes. Furthermore, we provide experimental evidence to indicate that sulforaphane-induced autophagy inhibits cytosolic release of cytochrome *c* and apoptotic cell death in prostate cancer cells. This is the first description to indicate induction of autophagy as a defense mechanism against apoptotic cell death by an isothiocyanate class of dietary chemopreventive agent.

Requests for reprints: Shivendra V. Singh, 2.32A Hillman Cancer Center Research Pavilion, University of Pittsburgh Cancer Institute, 5117 Centre Avenue, Pittsburgh, PA 15213. Phone: 412-623-3263; Fax: 412-623-7828; E-mail: singhs@upmc.edu.

doi:10.1158/0008-5472.CAN-06-0139

Materials and Methods

Reagents. D,L-Sulforaphane (purity > 99 %) was purchased from LKT Laboratories (St. Paul, MN). Tissue culture medium, penicillin/streptomycin antibiotic mixture, and fetal bovine serum (FBS) were from Life Technologies (Grand Island, NY), propidium iodide, 4′,6-diamidino-2-phenylindole (DAPI), 3-methyladenine (3-MA), and acridine orange were from Sigma (St. Louis, MO), RNase A was from Promega (Madison, WI) and the kit for quantitation of cytoplasmic histone–associated DNA fragmentation was from Roche Diagnostics (Mannheim, Germany). The antibody against LC3 was from Santa Cruz Biotechnology (Santa Cruz, CA), the anti–cytochrome *c* antibody was from BD PharMingen (San Diego, CA), and antiactin antibody was from Oncogene Research Products (San Diego, CA).

Cell lines and cell culture. Monolayer cultures of PC-3 cells were maintained in F-12K nutrient mixture (Kaighn's modification) supplemented with 7% (v/v) non–heat-inactivated FBS and antibiotics. PC-3 cells stably expressing green fluorescence protein (GFP)-tagged LC3 (GFP-LC3) were generated by transfection with pGFP-LC3 plasmid, kindly provided by Dr. Tamotsu Yoshimori (National Institute of Genetics, Shizuoka-ken, Japan), using LipofectAMINE 2000 (Invitrogen, Carlsbad, CA) and selection on 800 μg/mL G418. LNCaP cells were cultured in RPMI 1640 supplemented with 10% (v/v) non–heat-inactivated FBS, 10 mmol/L HEPES, 1 mmol/L sodium pyruvate, 0.2% glucose, and antibiotics. Each cell line was maintained at 37°C in an atmosphere of 95% air and 5% CO_2. Stock solution of sulforaphane was prepared in DMSO and an equal volume of DMSO was added to the controls.

Transmission electron microscopy. Transmission electron microscopy to determine the effect of sulforaphane treatment on ultrastructure of PC-3 and LNCaP cells was done essentially as described by Watkins and Cullen (22). Briefly, PC-3 or LNCaP cells (2×10^5) were plated in six-well plates and allowed to attach overnight. The cells were then treated with either DMSO (control) or 40 μmol/L sulforaphane for 6, 9, or 16 hours at 37°C. The cells were fixed in ice-cold 2.5% electron microscopy grade glutaraldehyde in PBS (pH 7.3). The specimens were rinsed with PBS, postfixed in 1% osmium tetroxide with 0.1% potassium ferricyanide, dehydrated through a graded series of ethanol (30-90%), and embedded in Epon (dodecenyl succinic anhydride, nadic methyl anhydride, scipoxy 812 resin, and dimethylaminomethyl; Energy Beam Sciences, Agawam, MA). Semithin (300 nm) sections were cut using a Reichart Ultracut, stained with 0.5% toluidine blue, and examined under a light microscope. Ultrathin sections (65 nm) were stained with 2% uranyl acetate and Reynold's lead citrate, and examined on a JEOL 1210 transmission electron microscope at ×10,000 or ×50,000 magnification.

Detection of AVOs. PC-3 or LNCaP cells (1×10^5) were plated on coverslips and allowed to attach. Following treatment with DMSO (control) or 40 μmol/L sulforaphane for specified time periods, cells were stained with 1 μg/mL acridine orange for 15 minutes, washed with PBS, and examined under a Leica fluorescence microscope at ×100 objective lens magnification.

Immunocytochemistry for LC3 localization. PC-3 or LNCaP cells (1×10^5) were grown on coverslips and allowed to attach by overnight incubation. The cells were then exposed to DMSO or 40 μmol/L sulforaphane for desired time period at 37°C, washed with PBS, and fixed at 4°C overnight using 2% paraformaldehyde. Subsequently, the cells were permeabilized with 0.1% Triton X-100 for 15 minutes at room temperature, washed with PBS, and blocked with PBS containing 0.5% (w/v) bovine serum albumin (BSA) and 0.15% (w/v) glycine (BSA buffer) for 1 hour at room temperature. Cells were treated with anti-LC3 (1: 50 dilution in BSA buffer) antibody for 1 hour at room temperature. Cells were then washed with BSA buffer and incubated with 2 μg/mL Alexa Fluor 488–conjugated goat anti-rabbit antibody (Molecular Probes, Eugene, OR) for 1 hour at room temperature. Slides were mounted and examined under a Leica fluorescence microscope.

Immunoblotting. Cells were treated with sulforaphane as described above and lysed using a solution containing 50 mmol/L Tris, 1% Triton X-100, 0.1% SDS, 150 mmol/L NaCl, protease inhibitor cocktail, 20 mmol/L Na_3VO_4, 20 mmol/L EGTA, 12 mmol/L α-glycerol phosphate, and 10 mmol/L NaF. The lysate was cleared by centrifugation at 14,000 rpm for 15 minutes. Lysate proteins were resolved by SDS-PAGE and transferred onto polyvinylidene difluoride membrane. The membrane was treated with a solution containing 10 mmol/L Tris (pH 7.4), 150 mmol/L NaCl, 0.05% Tween 20 and 5% nonfat dry milk, and incubated with the desired primary antibody for 2 hours at room temperature. The membrane was treated with appropriate secondary antibody for 1 hour at room temperature. The immunoreactive bands were visualized by enhanced chemiluminescence method. The blots were stripped and reprobed with antiactin antibody to normalize for differences in protein loading. The intensity of the immunoreactive bands was determined by densitometric scanning to quantify changes in protein levels.

Apoptosis assay. Apoptosis induction by sulforaphane was assessed by (*a*) flow cytometric analysis of cells with sub-G_0-G_1 DNA content (subdiploid cells) following staining with propidium iodide and (*b*) analysis of cytoplasmic histone–associated DNA fragmentation using a commercially available ELISA kit. For analysis of subdiploid cells, cells were treated with DMSO or sulforaphane in the absence or presence of 10 mmol/L 3-MA. Both floating and attached cells were collected, washed with PBS, fixed with 70% ethanol, and incubated for 30 minutes at room temperature with propidium iodide and RNase A. Stained cells were analyzed using a Coulter Epics XL Flow Cytometer as described by us previously (18). Cytoplasmic histone–associated DNA fragmentation was determined as suggested by the manufacturer.

Immunocytochemistry for cytochrome *c* localization. PC-3 cells were grown on coverslips, and exposed to DMSO or 40 μmol/L sulforaphane in the absence or presence of 10 mmol/L 3-MA for 9 hours at 37°C. The cells were stained with MitoTracker Red (CM-H_2XRos; Molecular Probes) diluted 1:5,000 in complete medium at 37°C for 30 minutes. The cells were kept in fresh medium for 30 minutes and fixed with 2% paraformaldehyde. Immunostaining was done as described above except that anti–cytochrome *c* antibody was used (1:2,000 dilution) and the cells were treated with 2 μg/mL Alexa Fluor 488–conjugated goat anti-mouse antibody (Molecular Probes). After washing with PBS, the cells were counterstained with 10 ng/mL DAPI and examined under a Leica fluorescence microscope at ×100 objective lens magnification.

Results and Discussion

Electron microscopy revealed formation of autophagosomes in sulforaphane-treated PC-3 cells. We have shown previously that sulforaphane-induced apoptosis in PC-3 cells is initiated by mitochondria-mediated and nonmitochondrial generation of reactive oxygen species leading to disruption of the mitochondrial membrane potential and release of cytochrome *c* from mitochondria to the cytosol (20). The release of cytochrome *c* and apoptosis induction in PC-3 cells was clearly evident by 16 hours of treatment with sulforaphane (20). Sulforaphane-induced disruption of the mitochondrial membrane potential, cytosolic release of cytochrome *c*, and apoptosis was significantly attenuated on pretreatment with small-molecule antioxidants or by adenovirus-mediated transduction of catalase (20). Because mitochondria with altered membrane potential and active in reactive oxygen species production are especially sensitive to autophagy (23, 24), which is a dynamic process for degradation and turnover of cytoplasmic organelles, including mitochondria (reviewed in refs. 25, 26), we hypothesized that sulforaphane may cause autophagy. We tested this hypothesis by examining the ultrastructures of control and sulforaphane-treated PC-3 cells by transmission electron microscopy. As can be seen in Fig. 1, DMSO-treated control PC-3 cells exhibited large nuclei with uniform and fine dispersed chromatin surrounded by cytoplasm with a normal complement of healthy-looking mitochondria at all three time points. Electron microscopy of PC-3 cells treated for 6 hours with sulforaphane revealed the appearance of large membranous

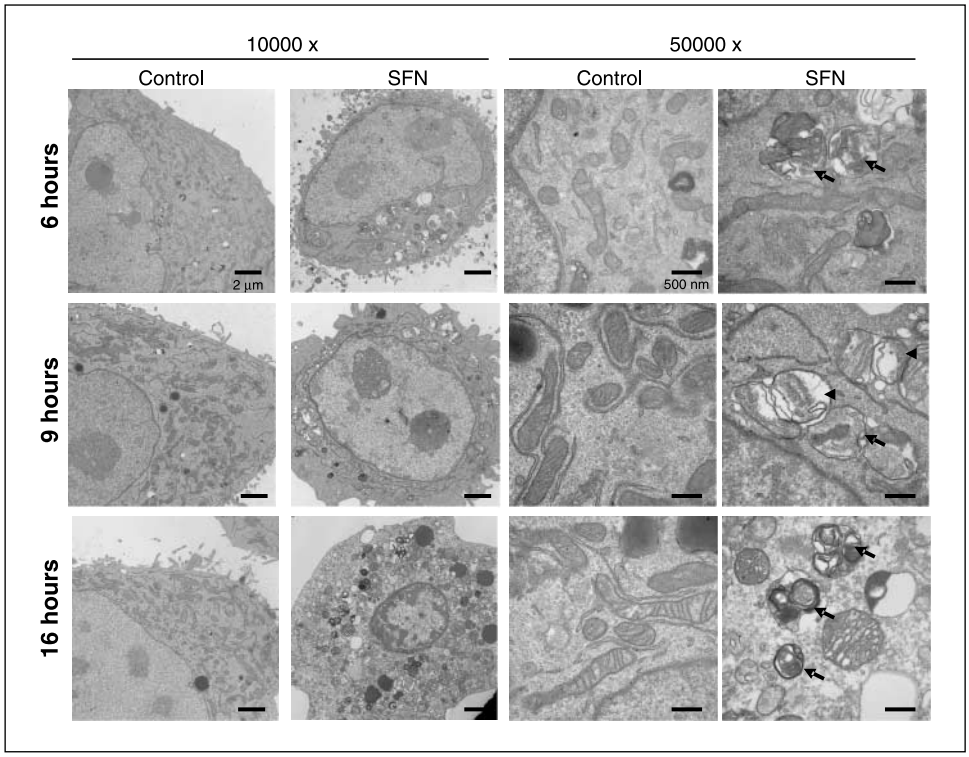

Figure 1. Representative transmission electron micrographs depicting ultrastructures of PC-3 cells treated with DMSO or 40 μmol/L sulforaphane (*SFN*) for the indicated time periods. Note the abundance of membranous vacuoles (*arrows*) in sulforaphane-treated PC-3 cells, which were rarely seen in DMSO-treated controls. Some of these vacuoles contained remnants of organelles, including mitochondria (*arrowhead*). Morphologic features of apoptosis (chromatin condensation and DNA fragmentation) were also evident in PC-3 cells treated for 16 hours with sulforaphane. Bars, 2 μm (×10,000 magnification) and 500 nm (×50,000 magnification).

vacuoles in the cytoplasm, but the nuclei of these cells appeared normal with minimum evidence of chromatin condensation. The formation of these membranous vacuoles increased progressively with increasing sulforaphane exposure time. Some of the vacuoles resembled autophagosomes and contained remnants of degraded organelles, including mitochondria (Fig. 1, *right, arrowhead*). The cytoplasm of PC-3 cells treated for 16 hours with sulforaphane was full of membranous vacuoles and the nuclei exhibited chromatin condensation, a characteristic feature of cells undergoing apoptosis (Fig. 1). These results indicated that sulforaphane treatment caused formation of autophagosome-like structures in PC-3 cells and this cellular response occurred before the onset of apoptosis.

Sulforaphane treatment caused formation of AVOs. Formation of AVOs is another characteristic feature of cells engaged in autophagy following treatment with different stimuli, including radiation or ceramide (27, 28). We therefore determined the effect of sulforaphane treatment on formation of AVOs in PC-3 cells by fluorescence microscopy following staining with the lysosomotropic agent acridine orange (Fig. 2*A*). Acridine orange is a weak base that is able to move freely across biological membranes in an uncharged state characterized by green fluorescence. The protonated form of acridine orange accumulates in acidic compartments and forms aggregates, which is characterized by red fluorescence. As can be seen in Fig. 2*A*, DMSO-treated control PC-3 cells displayed primarily green fluorescence with minimal red fluorescence, indicating a lack of AVOs. On the other hand, treatment of PC-3 cells with 40 μmol/L sulforaphane resulted in formation of red fluorescent AVOs that were relatively more pronounced at 16 hours posttreatment compared with 6-hour time point. These results provided further evidence to indicate that sulforaphane treatment caused autophagy in PC-3 cells.

Involvement of LC3 in sulforaphane-induced autophagy. To gain insights into the mechanism of sulforaphane-induced autophagy, we examined the effect of sulforaphane treatment on LC3, which is the mammalian homologue of yeast autophagy protein Apg8/Aut7p (28, 29). LC3 exists as two forms—an 18 kDa cytosolic protein (LC3-I) and a processed 16 kDa form (LC3-II) in cells engaged in autophagy (30). Studies have also revealed that the LC3-II form is mainly localized in autophagosome membranes (30). To test the involvement of LC3 in sulforaphane-induced autophagy, we initially determined the effect of sulforaphane treatment on localization of LC3 by immunofluorescence microscopy and the results are shown in Fig. 2*B*. The DMSO-treated control PC-3 cells (6 or 16 hours) exhibited diffuse distribution of LC3-associated green fluorescence. On the other hand, PC-3 cells treated for 6 and 16 hours with sulforaphane displayed a punctate pattern of LC3 immunostaining with increased fluorescence, which characterizes its redistribution to autophagosomes (Fig. 2*B*). To confirm involvement of LC3 in sulforaphane-induced autophagy, we generated stable transfectants of PC-3 cells expressing GFP-LC3 (30). Fluorescence microscopy revealed a diffuse localization of GFP-LC3 in DMSO-treated control cells (Fig. 3*A*). By contrast, treatment of cells with 40 μmol/L sulforaphane for 6 hours produced a punctate pattern for GFP-LC3 fluorescence, indicating recruitment of LC3-II to autophagosomes during sulforaphane-induced autophagy (Fig. 3*A*).

Next, we tested whether sulforaphane treatment caused processing of full-length LC3-I (18 kDa) to LC3-II (16 kDa) by performing immunoblotting using lysates from PC-3 cells treated with either DMSO (control) or 40 μmol/L sulforaphane for 6, 9, and 16 hours (Fig. 3*B*). Lysates from DMSO-treated control PC-3 cells exhibited predominantly an 18 kDa band representing LC3-I. An immunoreactive band corresponding to processed LC3-II (16 kDa) was either not detectable (6-hour time point) or present with a weak intensity (9- and 16-hour time points) in DMSO-treated control lysates. On the other hand, immunoblotting using

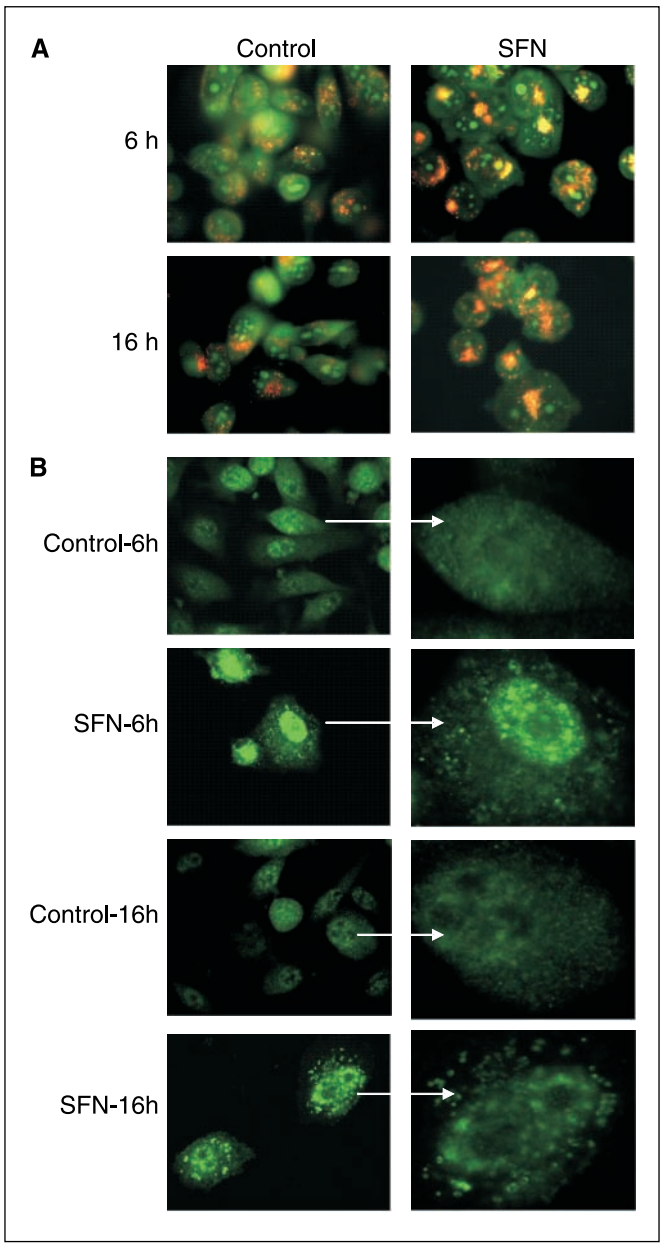

Figure 2. *A,* fluorescence microscopic analysis for acridine orange staining in PC-3 cells treated for 6 or 16 hours with DMSO (control) or 40 μmol/L sulforaphane. Note the formation of acridine orange–accumulating AVOs (*orange-red fluorescence*) in sulforaphane-treated PC-3 cells. *B,* immunocytochemistry for LC3 localization in PC-3 cells treated for 6 or 16 hours with DMSO (control) or 40 μmol/L sulforaphane. The DMSO-treated control PC-3 cells exhibited diffuse distribution of LC3-associated green fluorescence, whereas sulforaphane-treated cells displayed a punctate pattern of LC3 immunostaining with increased fluorescence. *Right,* enlarged images of the cells marked by arrows. Similar results were observed in replicate experiments.

lysates from sulforaphane-treated PC-3 cells revealed the presence of processed LC3-II that was evident as early as 6 hours posttreatment and its intensity increased with longer treatment times. In addition, sulforaphane treatment caused a marked increase in the level of LC3-I protein especially at the 9- and 16-hour time points compared with vehicle-treated control (Fig. 3*B*). Collectively, these results indicated that the sulforaphane-induced autophagy in PC-3 cells was associated with induction as well as processing of LC3-I to promote redistribution of LC3-II to autophagosomes.

Autophagy inhibited sulforaphane-induced apoptosis. Next, we raised the question whether induction of autophagy affects sulforaphane-induced cell death. We addressed this question using 3-MA, a specific inhibitor of autophagy (31). The sulforaphane-induced redistribution of LC3-II to autophagosomes was significantly attenuated in the presence of 10 mmol/L 3-MA as revealed by immunofluorescence microscopy for LC3 localization (data not shown). The effect of 3-MA on sulforaphane-induced apoptosis was determined by analysis of subdiploid cells by flow cytometry following staining with propidium iodide. Representative flow histograms for PC-3 cultures treated for 16 hours with either DMSO or 40 μmol/L sulforaphane in the presence or absence of 3-MA are shown in Fig. 4*A*. Sulforaphane treatment caused a nearly 6-fold increase in the percentage of apoptotic cells with sub-G_0-G_1 DNA content compared with DMSO-treated control. Importantly, sulforaphane-induced apoptosis was exacerbated in the presence of 3-MA, whereas 3-MA treatment alone did not cause accumulation of subdiploid cells (Fig. 4*B*). The percentage of apoptotic cells with sub-G_0-G_1 DNA content was increased by ~2.3-fold upon cotreatment of PC-3 cells with sulforaphane and 3-MA when compared with sulforaphane treatment alone ($P < 0.05$ by one-way ANOVA followed by Bonferroni's multiple comparison test; Fig. 4*B*). The 3-MA-mediated exacerbation of sulforaphane-induced apoptosis was confirmed by analysis of cytoplasmic histone–associated

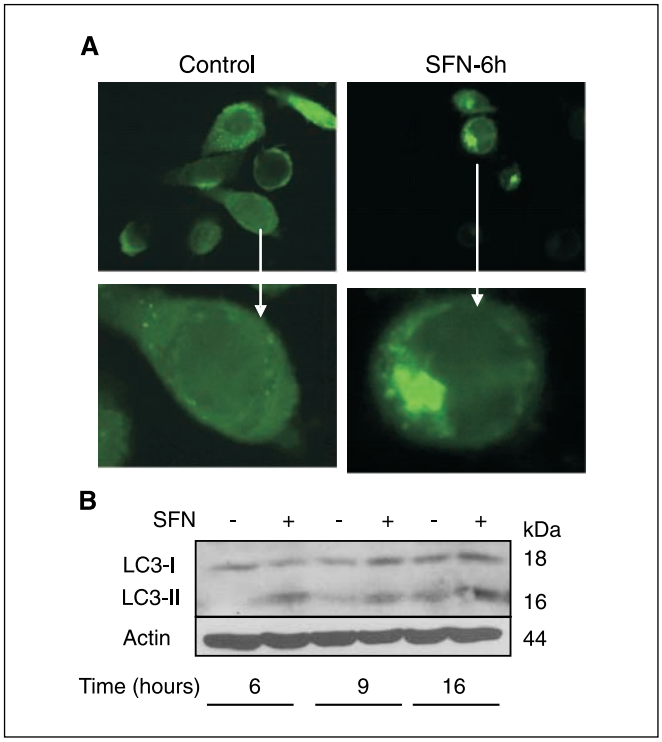

Figure 3. *A,* GFP fluorescence in PC-3 cells stably transfected with GFP-LC3 following a 6-hour treatment with DMSO or 40 μmol/L sulforaphane. In DMSO-treated control PC-3 cells, GFP-LC3 was diffusely and uniformly distributed. By contrast, sulforaphane treatment caused redistribution of GFP-LC3 to autophagosomes. *Bottom,* enlarged images of the cells marked by arrows. *B,* immunoblotting for LC3-I and LC3-II using lysates from PC-3 cells treated for 6, 9, or 16 hours with either DMSO (control) or 40 μmol/L sulforaphane. The blots were stripped and reprobed with antiactin antibody to ensure equal protein loading. Similar results were observed in at least two independent experiments.

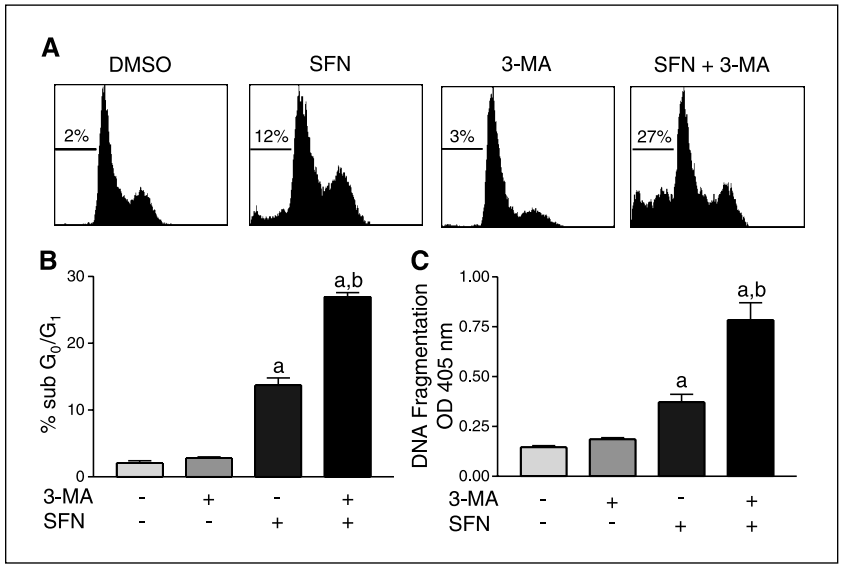

Figure 4. *A,* representative flow histograms depicting subdiploid fraction in PC-3 cultures treated for 16 hours with DMSO (control) or 40 μmol/L sulforaphane in the presence or absence of 10 mmol/L 3-MA. Note a >2-fold increase in subdiploid cells in PC-3 cultures treated with sulforaphane plus 3-MA compared with sulforaphane treatment alone. *B,* percentage of subdiploid cells in PC-3 cultures treated for 16 hours with DMSO or 40 μmol/L sulforaphane in the presence or absence of 10 mmol/L 3-MA. *C,* cytoplasmic histone–associated DNA fragmentation in PC-3 cells treated for 24 hours with DMSO (control) or 20 μmol/L sulforaphane in the presence or absence of 10 mmol/L 3-MA. *Columns* (*B* and *C*), mean ($n = 3–4$); *bars*, SE. a, $P < 0.05$, significantly different compared with DMSO-treated control; b, $P < 0.05$, significantly different compared with sulforaphane-alone treatment group by one-way ANOVA followed by Bonferroni's multiple comparison test. Similar results were observed in replicate experiments.

DNA fragmentation, which has emerged as a sensitive technique for quantitation of apoptosis. As can be seen in Fig. 4*C*, cytoplasmic histone–associated DNA fragmentation was statistically significantly higher in PC-3 cells cotreated with 3-MA and sulforaphane compared with that observed on treatment with sulforaphane alone ($P < 0.05$ by one-way ANOVA followed by Bonferroni's multiple comparison test). In agreement with the results of subdiploid cell analysis, 3-MA treatment alone did not cause cytoplasmic histone–associated DNA fragmentation. Collectively, these results indicated that sulforaphane-induced autophagy inhibits apoptosis in our model.

3-MA promoted sulforaphane-induced release of cytochrome *c*. The results of the apoptosis assays described above raised the question of whether autophagy prevented sulforaphane-induced cytosolic release of cytochrome *c* due to sequestration of mitochondria in autophagosomes. To address this question, we determined the effect of sulforaphane ± 3-MA treatments on cytochrome *c* release by immunocytochemistry and the results are shown in Fig. 5. The cytochrome *c* in PC-3 cells treated for 9 hours with DMSO alone or 3-MA alone was largely localized in mitochondria, as revealed by a yellow-orange staining around DAPI-stained nuclei (blue fluorescence). The yellow-orange staining was due to the merging of red fluorescence (MitoTracker Red) derived from mitochondria and cytochrome *c*–associated green fluorescence. Sulforaphane treatment alone caused translocation of cytochrome *c* from mitochondria to the cytosol, which was evidenced by the appearance of green fluorescence in the cytoplasm (marked by an arrow in panel representing sulforaphane treatment alone). This cytochrome *c*–associated green fluorescence was considerably more pronounced in PC-3 cells treated with sulforaphane plus 3-MA. These results indicated that inhibition of autophagy by 3-MA potentiated sulforaphane-mediated release of cytochrome *c*.

Sulforaphane-induced autophagy was not restricted to PC-3 cells. Next, we raised the question of whether sulforaphane-induced autophagy was restricted to PC-3 cells due to its unique genetic background. To address this question, we used another well-characterized human prostate cancer cell line, LNCaP. Unlike PC-3 cells, the LNCaP cell line is androgen-responsive and contains wild-type p53. Similar to PC-3 cells, however, treatment of LNCaP cells with 40 μmol/L sulforaphane resulted in formation of membranous autophagosome-like structures that were evident as early as 6 hours after treatment (Fig. 6*A*) and increased gradually with increasing treatment times (results not shown). In addition, sulforaphane treatment (40 μmol/L for 6 hours) caused formation of AVOs as revealed by vital acridine orange staining (Fig. 6*B*), whereas AVOs were less visible in DMSO-treated control LNCaP

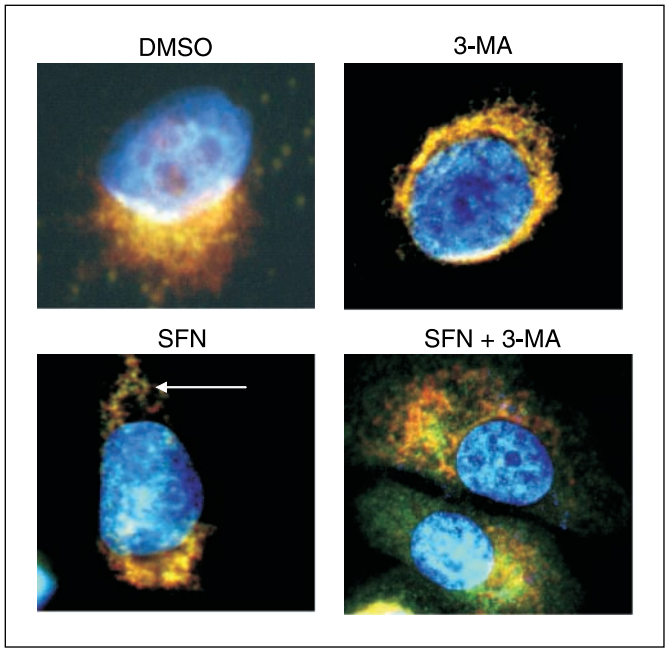

Figure 5. Immunocytochemistry for cytochrome *c* localization in PC-3 cells treated for 9 hours with DMSO (control) or 40 μmol/L sulforaphane in the presence or absence of 10 mmol/L 3-MA. Staining for cytochrome *c* (*green fluorescence*), MitoTracker Red (mitochondria; *red fluorescence*), and DAPI (nuclei; *blue fluorescence*). In cells treated with DMSO or 3-MA alone, cytochrome *c* was primarily localized in mitochondria as revealed by a yellow-orange staining due to merging of red (mitochondria) and green fluorescence (cytochrome *c*). Sulforaphane treatment alone caused translocation of cytochrome *c* from mitochondria to the cytosol evidenced by appearance of green fluorescence in the cytoplasm (*arrow*). Cytosolic cytochrome *c* (*green fluorescence*) was much more pronounced in PC-3 cells treated with sulforaphane plus 3-MA. Similar results were observed in replicate experiments.

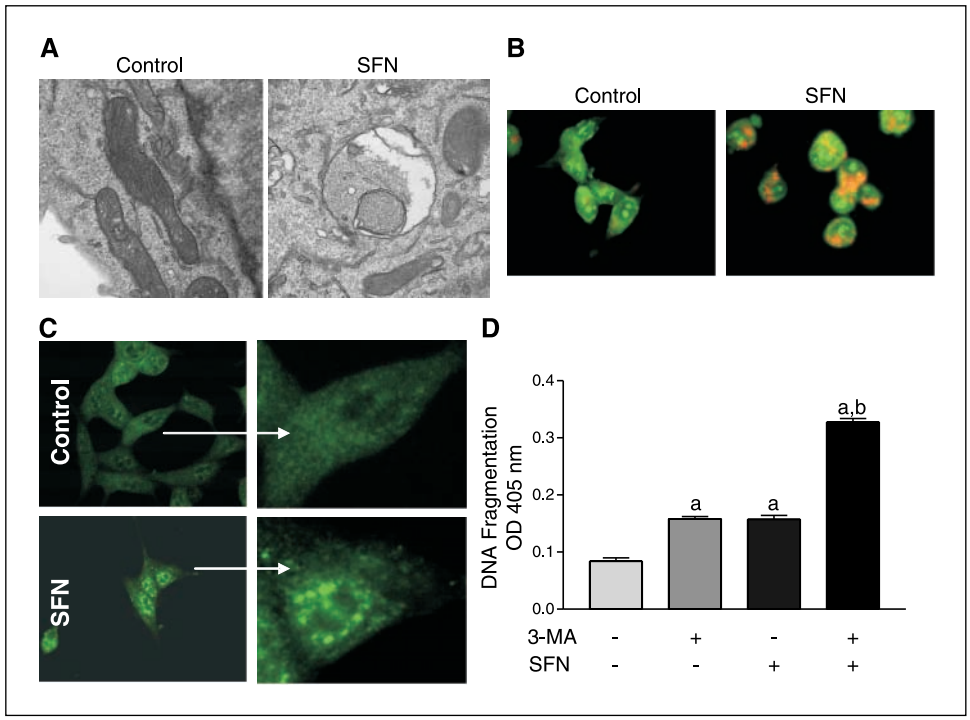

Figure 6. *A,* representative electron micrographs depicting ultrastructures of LNCaP cells treated for 6 hours with DMSO or 40 μmol/L sulforaphane. Note the healthy-looking mitochondria in control cells and membranous vacuoles in sulforaphane-treated LNCaP cells. Magnification, ×50,000. *B,* acridine orange staining in LNCaP cells treated for 6 hours with either DMSO (control) or 40 μmol/L sulforaphane. Similar results were observed in two independent experiments. *C,* immunocytochemistry for LC3 localization in LNCaP cells treated for 6 hours with DMSO or 40 μmol/L sulforaphane. *Right,* enlarged images of the cells marked by arrows. *D,* cytoplasmic histone–associated DNA fragmentation in LNCaP cells treated with DMSO (control) or 10 μmol/L sulforaphane in the presence or absence of 10 mmol/L 3-MA. *Columns,* mean ($n = 3$); *bars*, SE. a, $P < 0.05$, significantly different compared with DMSO-treated control; b, $P < 0.05$, significantly different compared with sulforaphane-alone treatment group by one-way ANOVA followed by Bonferroni's multiple comparison test. Similar results were observed in replicate experiments.

cells (Fig. 6*B*). Immunostaining for LC3 localization confirmed the induction of autophagy in LNCaP cells treated with sulforaphane characterized by punctate pattern of LC3 distribution to autophagosomes (Fig. 6*C*). Finally, similar to PC-3 cells, sulforaphane-induced accumulation of subdiploid cells (data not shown) and cytoplasmic histone–associated DNA fragmentation (Fig. 6*D*) were significantly increased in the presence of the autophagy inhibitor 3-MA. Collectively, these results indicated that sulforaphane-induced autophagy was a generalized phenomenon and not restricted to PC-3 cells.

The present study provides experimental evidence to show, for the first time, activation of an autophagic program in human prostate cancer cells on treatment with sulforaphane, which is a highly promising cancer chemopreventive constituent of many edible cruciferous vegetables (5–10). Sulforaphane-mediated autophagy in PC-3 and LNCaP human prostate cancer cells is characterized by the appearance of membranous vacuoles containing remnants of mitochondria, formation of AVOs, induction of LC3-I, and recruitment of processed LC3-II to autophagosomes. We also show that the sulforaphane-induced morphologic and biochemical changes associated with autophagy precede the onset of apoptosis. For example, sulforaphane-induced formation of membranous vacuoles and AVOs is evident as early as 6 hours after treatment and increases progressively with increasing treatment time, but, as reported previously (20) the morphologic (e.g., chromatin condensation and DNA fragmentation) and biochemical features [e.g., cytosolic release of cytochrome *c* and proteolytic cleavage of procaspase-3 and poly(ADP-ribose)polymerase] characteristic of apoptosis are not observed until 16 hours posttreatment.

Autophagy is an evolutionary conserved, dynamic, and lysosome-mediated process that begins with the formation of double or multilayer membranous structures and is induced by poor nutrient conditions (25, 26, 31). During autophagy, the cytoplasmic components, including organelles, such as mitochondria, are engulfed by the membranous vacuoles often called autophagosomes, which fuse with lysosomes where the contents are degraded by the lysosomal proteases (25, 26, 31). Autophagic response has been observed in response to various cancer-relevant stimuli, including Ras activation (32), nutrient deprivation (33), and treatment with endostatin (34), radiation (27), tumor necrosis factor-α (TNF-α; ref. 35), ceramide (28), rapamycin (36), arsenic trioxide (37), or tamoxifen (38). Autophagy is shown to be cytotoxic by some of these stimuli (e.g., ceramide and rapamycin) and this form of cell death (called type II cell death) is distinct from apoptotic type I cell death (28, 36). Although the connection between autophagy and apoptotic cell death is not clear, autophagy seems to promote apoptosis in some systems. For example, the formation of autophagosomes has been shown to be associated with TNF-α-induced apoptosis in human T lymphoblastic leukemia cells (35). In this model, inhibition of autophagy by 3-MA also inhibits DNA fragmentation (35). The present study reveals that autophagy represents a defense mechanism against sulforaphane-induced apoptosis in human prostate cancer cells. This conclusion is based on the observations that sulforaphane-induced release of cytochrome *c* as well as apoptosis induction were significantly exacerbated in the presence of the autophagy inhibitor 3-MA. Thus, it is reasonable to postulate that sulforaphane-induced autophagy sequesters mitochondria in autophagosomes resulting in delayed release of cytochrome *c* and activation of intrinsic caspase cascade.

Apoptosis induction by certain sulforaphane analogues (e.g., phenethyl isothiocyanate) is regulated by p53 in some cellular systems (14, 39). For instance, mouse embryonic fibroblasts lacking p53 are resistant to phenethyl isothiocyanate–induced apoptosis compared with fibroblasts derived from wild-type mice (39). The present study suggests that p53 may not be required for sulforaphane-induced autophagy or apoptosis because both PC-3 cells, which lack functional p53, and LNCaP cells expressing wild-type p53 are sensitive to sulforaphane-induced autophagy as well as apoptosis.

Formation of autophagosomes is a complex process regulated by multiple molecules (reviewed in refs. 40–42). For example, a conjugation system involving Atg7 and Atg3 is responsible for addition of a phospholipid moiety to LC3-I to trigger its membrane localization. Likewise, autophagy is regulated by type III phosphatidylinositol 3-kinase (PI3K) complex containing beclin-1 (43). Type III PI3K complex is the putative target of 3-MA (43). Although we have not determined the effect of sulforaphane on beclin-1 protein, inhibition of sulforaphane-induced autophagy in the presence of 3-MA points toward involvement of type III PI3K in autophagic program in our model. Beclin-1 was identified in a yeast two-hybrid screen as a Bcl-2-interacting protein (44). Recently, it was shown that Bcl-2, by binding to beclin-1, disrupts its autophagy function (45). Agents capable of disrupting the interaction between Bcl-2 and beclin-1 are likely to promote autophagy. We have shown previously that sulforaphane treatment causes a reduction in Bcl-2 protein level in PC-3 cells (20), which is likely to relieve beclin-1. Thus, it is possible that sulforaphane-induced autophagy is promoted by disruption of the interaction between Bcl-2 and beclin-1. Mammalian target of rapamycin (mTOR) is also implicated in regulation of autophagy (46). Inhibition of *Saccharomyces cerevisiae* TOR increases level of Atg8 (LC3) and the kinase activity of Atg1 (42, 47). Because we observed up-regulation and processing of LC3 on treatment with sulforaphane (Fig. 3), the possibility that sulforaphane targets mTOR to trigger autophagy cannot be ruled out. However, additional experiments are required to systematically explore this possibility. Activation of extracellular signal-regulated kinase 1/2 (ERK1/2) has been shown to stimulate autophagy in human colon cancer cells (48, 49). Although sulforaphane treatment causes activation of ERK1/2 in PC-3 cells, an inhibitor of ERK1/2 activation (PD98059) fails to protect against sulforaphane-mediated processing and redistribution to autophagosomes of LC3 (data not shown). These results suggest that ERK1/2 may not be involved in sulforaphane-induced autophagy in our model.

In conclusion, the present study reveals that apoptosis induction by sulforaphane in PC-3 and LNCaP human prostate cancer cells is prevented by induction of autophagy. This is the first published report to document activation of an autophagic program in the context of apoptosis by an isothiocyanate class of anticancer agent. It is reasonable to speculate that the cancer chemopreventive activity of sulforaphane may be enhanced by the simultaneous treatment with an inhibitor of autophagy.

Acknowledgments

Received 1/13/2006; revised 2/27/2006; accepted 3/14/2006.

Grant support: USPHS grants CA115498 and CA101753, awarded by the National Cancer Institute.

The costs of publication of this article were defrayed in part by the payment of page charges. This article must therefore be hereby marked *advertisement* in accordance with 18 U.S.C. Section 1734 solely to indicate this fact.

We thank Dr. Tamotsu Yoshimori for generous gift of GFP-LC3 plasmid and Karen L. Lew for technical assistance.

References

1. Verhoeven DT, Goldbohm RA, van Poppel G, Verhagen H, van den Brandt PA. Epidemiological studies on *Brassica* vegetables and cancer risk. Cancer Epidemiol Biomarkers Prev 1996;5:733–48.
2. Cohen JH, Kristal AR, Stanford JL. Fruit and vegetable intakes and prostate cancer risk. J Natl Cancer Inst 2000; 92:61–8.
3. Zhang SM, Hunter DJ, Rosner BA, et al. Intakes of fruits, vegetables, and related nutrients and the risk of non-Hodgkin's lymphoma among women. Cancer Epidemiol Biomarkers Prev 2000;9:477–85.
4. Ambrosone CB, McCann SE, Freudenheim JL, Marshall JR, Zhang Y, Shields PG. Breast cancer risk in premenopausal women is inversely associated with consumption of broccoli, a source of isothiocyanates, but is not modified by GST genotype. J Nutr 2004;134: 1134–8.
5. Hecht SS. Inhibition of carcinogenesis by isothiocyanates. Drug Metab Rev 2000;32:395–411.
6. Fahey JW, Zalcmann AT, Talalay P. The chemical diversity and distribution of glucosinolates and isothiocyanates among plants. Phytochemistry 2001; 56:5–51.
7. Zhang Y, Talalay P, Cho CG, Posner GH. A major inducer of anticarcinogenic protective enzymes from broccoli: isolation and elucidation of structure. Proc Natl Acad Sci U S A 1992;89:2399–403.
8. Zhang Y, Kensler TW, Cho CG, Posner GH, Talalay P. Anticarcinogenic activities of sulforaphane and structurally related synthetic norbornyl isothiocyanates. Proc Natl Acad Sci U S A 1994;91:3147–50.
9. Chung FL, Conaway CC, Rao CV, Reddy BS. Chemoprevention of colonic aberrant crypt foci in Fischer rats by sulforaphane and phenethyl isothiocyanate. Carcinogenesis 2000;21:2287–91.
10. Fahey JW, Haristoy X, Dolan PM, et al. Sulforaphane inhibits extracellular, intracellular, and antibiotic-resistant strains of *Helicobacter pylori* and prevents benzo (*a*)pyrene-induced stomach tumors. Proc Natl Acad Sci U S A 2002;99:7610–5.
11. Brooks JD, Paton VG, Vidanes G. Potent induction of phase 2 enzymes in human prostate cells by sulforaphane. Cancer Epidemiol Biomarkers Prev 2001;10: 949–54.
12. Barcelo S, Gardiner JM, Gescher A, Chipman JK. CYP2E1-mediated mechanism of anti-genotoxicity of the broccoli constituent sulforaphane. Carcinogenesis 1996;17:277–82.
13. Gamet-Payrastre L, Li P, Lumeau S, et al. Sulforaphane, a naturally occurring isothiocyanate, induces cell cycle arrest and apoptosis in HT29 human colon cancer cells. Cancer Res 2000;60:1426–33.
14. Fimognari C, Nüsse M, Cesari R, Iori R, Cantelli-Forti G, Hrelia P. Growth inhibition, cell-cycle arrest and apoptosis in human T-cell leukemia by the isothiocyanate sulforaphane. Carcinogenesis 2002;23: 581–6.
15. Wang L, Liu D, Ahmed T, Chung FL, Conaway CC, Chiao JW. Targeting cell cycle machinery as a molecular mechanism of sulforaphane in prostate cancer prevention. Int J Oncol 2004;24:187–92.
16. Jackson SJT, Singletary KW. Sulforaphane: a naturally occurring mammary carcinoma mitotic inhibitor, which disrupts tubulin polymerization. Carcinogenesis 2004;25: 219–27.
17. Singh AV, Xiao D, Lew KL, Dhir R, Singh SV. Sulforaphane induces caspase-mediated apoptosis in cultured PC-3 human prostate cancer cells and retards growth of PC-3 xenografts *in vivo*. Carcinogenesis 2004; 25:83–90.
18. Singh SV, Herman-Antosiewicz A, Singh AV, et al. Sulforaphane-induced G_2/M phase cell cycle arrest involves checkpoint kinase 2 mediated phosphorylation of Cdc25C. J Biol Chem 2004;279:25813–22.
19. Choi S, Singh SV. Bax and Bak are required for apoptosis induction by sulforaphane, a cruciferous vegetable derived cancer chemopreventive agent. Cancer Res 2005;65:2035–43.
20. Singh SV, Srivastava SK, Choi S, et al. Sulforaphane-induced cell death in human prostate cancer cells is initiated by reactive oxygen species. J Biol Chem 2005; 280:19911–24.
21. Myzak MC, Karplus PA, Chung FL, Dashwood R. A novel mechanism of chemoprotection by sulforaphane: inhibition of histone deacetylase. Cancer Res 2004;64: 5767–74.
22. Watkins SC, Cullen MJ. A qualitative and quantitative study of the ultrastructure of regenerating muscle fibres in Duchenne muscular dystrophy and polymyositis. J Neurol Sci 1987;82:181–92.
23. de Grey ADNJ. A proposed refinement of the mitochondrial free radical theory of aging. Bioessays 1997;19:161–6.
24. Lemasters JJ, Nieminen AL, Qian T, et al. The mitochondrial permeability transition in cell death: a common mechanism in necrosis, apoptosis and autophagy. Biochim Biophys Acta 1998;1366:177–96.
25. Ogier-Denis E, Codogno P. Autophagy: a barrier or an adaptive response to cancer. Biochim Biophys Acta 2003;1603:113–28.
26. Lum JJ, DeBerardinis RJ, Thompson CB. Autophagy in metazoans: cell survival in the land of plenty. Nat Rev Mol Cell Biol 2005;6:439–48.
27. Paglin S, Hollister T, Delohery T, et al. A novel response of cancer cells to radiation involves autophagy and formation of acidic vesicles. Cancer Res 2001;61: 439–44.
28. Daido S, Kanzawa T, Yamamoto A, Takeuchi H, Kondo Y, Kondo S. Pivotal role of the cell death factor BNIP3 in ceramide-induced autophagic cell death in malignant glioma cells. Cancer Res 2004;64: 4286–93.
29. Kanzawa T, Germano IM, Komata T, Ito H, Kondo Y, Kondo S. Role of autophagy in temozolomide-induced cytotoxicity for malignant glioma cells. Cell Death Differ 2004;11:448–57.
30. Kabeya Y, Mizushima N, Ueno T, et al. LC3, a mammalian homologue of yeast Apg8p, is localized in autophagosome membranes after processing. EMBO J 2000;21:5720–8.
31. Seglen PO, Bohley P. Autophagy and other vacuolar protein degradation mechanisms. Experientia 1992;48: 158–72.
32. Chi S, Kitanaka C, Noguchi K, et al. Oncogenic Ras triggers cell suicide through the activation of a caspase-independent cell death program in human cancer cells. Oncogene 1999;18:2281–90.

33. Inbal B, Bialik S, Sabanay I, Shani G, Kimchi A. DAP kinase and DRP-1 mediate membrane blebbing and the formation of autophagic vesicles during programmed cell death. J Cell Biol 2002;157:455–68.

34. Chau YP, Lin SY, Chen JH, Tai MH. Endostatin induces autophagic cell death in EAhy926 human endothelial cells. Histol Histopathol 2003;18:715–26.

35. Jia L, Dourmashkin RR, Allen PD, Gray AB, Newland AC, Kelsey SM. Inhibition of autophagy abrogates tumour necrosis factor α induced apoptosis in human T-lymphoblastic leukaemic cells. Br J Haematol 1997;98: 673–85.

36. Takeuchi H, Kondo Y, Fujiwara K, et al. Synergistic augmentation of rapamycin-induced autophagy in malignant glioma cells by phosphatidylinositol 3-kinase/protein kinase B inhibitors. Cancer Res 2005; 65:3336–46.

37. Kanzawa T, Kondo Y, Ito H, Kondo S, Germano I. Induction of autophagic cell death in malignant glioma cells by arsenic trioxide. Cancer Res 2003;63:2103–8.

38. Bursch W, Ellinger A, Kienzl H, et al. Active cell death induced by the anti-estrogens tamoxifen and ICI 164 384 in human mammary carcinoma cells (MCF-7) in culture: the role of autophagy. Carcinogenesis 1996;17:1595–607.

39. Huang C, Ma WY, Hecht SS, Dong Z. Essential role of p53 in phenethyl isothiocyanate-induced apoptosis. Cancer Res 1998;58:4102–6.

40. Cuervo AM. Autophagy: many paths to the same end. Mol Cell Biochem 2004;263:55–72.

41. Ohsumi Y. Molecular dissection of autophagy: two ubiquitin-like systems. Nat Rev Mol Cell Biol 2001; 2:211–6.

42. Klionsky DJ. The molecular machinery of autophagy: unanswered questions. J Cell Sci 2005;118:7–18.

43. Kihara A, Kabeya Y, Ohsumi Y, Yoshimori T. Beclin-phosphatidylinositol 3-kinase complex functions at the trans-Golgi network. EMBO Rep 2001;2:330–5.

44. Liang XH, Kleeman LK, Jiang HH, et al. Protection against fatal Sindbis virus encephalitis by beclin, a novel Bcl-2-interacting protein. J Virol 1998;72:8586–96.

45. Pattingre S, Tassa A, Qu X, et al. Bcl-2 antiapoptotic proteins inhibit Beclin 1-dependent autophagy. Cell 2005;122:927–39.

46. Meijer AJ, Codogno P. Regulation and role of autophagy in mammalian cells. Int J Biochem Cell Biol 2004;36:2445–62.

47. Abeliovich H, Dunn WA, Kim J, Klionsky DJ. Dissection of autophagosome biogenesis into distinct nucleation and expansion steps. J Cell Biol 2000;151: 1025–34.

48. Ogier-Denis E, Pattingre S, El Benna J, Codogno P. Erk1/2-dependent phosphorylation of Gα-interacting protein stimulates its GTPase accelerating activity and autophagy in human colon cancer cells. J Biol Chem 2000;275:39090–5.

49. Ellington AA, Berhow MA, Singletary KW. Inhibition of Akt signaling and enhanced ERK1/2 activity are involved in induction of macroautophagy by triterpenoid B-group soyasaponins in colon cancer cells. Carcinogenesis 2006;27:298–306.